Review Article | Cardiovascular Imaging

eISSN 2005-8330
https://doi.org/10.3348/kjr.2020.1277
Korean J Radiol 2021;22(11):1749-1763

Korean Journal of Radiology
KJR

CT Assessment of Myocardial Perfusion and Fractional Flow Reserve in Coronary Artery Disease: A Review of Current Clinical Evidence and Recent Developments

Chun-Ho Yun[1], Chung-Lieh Hung[2, 3], Ming-Shien Wen[4], Yung-Liang Wan[5], Aaron So[6]

[1]Department of Radiology, MacKay Memorial Hospital, Taipei, Taiwan; [2]Division of Cardiology, Department of Internal Medicine, MacKay Memorial Hospital, Taipei, Taiwan; [3]Institute of Biomedical Sciences, Mackay Medical College, New Taipei, Taiwan; Departments of [4]Cardiology and [5]Medical Imaging and Intervention, Linkou Chang Gung Memorial Hospital, College of Medicine, Chang Gung University, Taoyuan, Taiwan; [6]Department of Medical Biophysics, University of Western Ontario, Imaging Program, Lawson Health Research Institute, London, Canada

Coronary computed tomography angiography (CCTA) is routinely used for anatomical assessment of coronary artery disease (CAD). However, invasive measurement of fractional flow reserve (FFR) is the current gold standard for the diagnosis of hemodynamically significant CAD. CT-derived FFRCT and CT perfusion are two emerging techniques that can provide a functional assessment of CAD for risk stratification and clinical decision making. Several clinical studies have shown that the diagnostic performance of concomitant CCTA and functional CT assessment for detecting hemodynamically significant CAD is at least non-inferior to that of other routinely used imaging modalities. This article aims to review the current clinical evidence and recent developments in functional CT techniques.

Keywords: *CT perfusion; CT fractional flow reserve; CT angiography; Coronary artery disease*

INTRODUCTION

Coronary computed tomography angiography (CCTA) has played an important role in the anatomic assessment of coronary artery disease (CAD) through direct non-invasive evaluation of coronary lumen narrowing (stenosis) and atherosclerotic plaques. CCTA has demonstrated excellent diagnostic accuracy in detecting obstructive CAD compared to invasive coronary angiography (ICA) [1-4]. In patients with a low-to-intermediate risk of CAD, a normal CCTA scan can rule out obstructive CAD due to its high negative predictive value [4]. However, the positive predictive value and specificity of CCTA are mediocre [1,2] due to the blooming and beam-hardening artifacts emanating from calcified plaques, which make image interpretation more difficult. In addition, similar to ICA, CCTA provides morphological assessment of the coronary arteries but cannot offer functional information regarding ischemia in the downstream myocardium, which is critical for decision-making on subsequent treatments, including optimal medical therapy and invasive revascularization interventions.

Single-photon emission computed tomography (SPECT) plays an essential role in detecting myocardial ischemia and provides robust prognostic information [5,6]. However, limitations such as being qualitative and low in spatial resolution have affected the diagnostic performance of SPECT in assessing balanced ischemia and differentiating between subendocardial and transmural perfusion defects. However, the most recent cardiology guidelines consider fractional flow reserve (FFR) as the gold standard for the functional assessment of CAD [7,8]. Consequently, cardiac imagers are keen to compare non-invasive functional imaging modalities with FFR. In this paper, we review three

Received: October 23, 2020 **Revised:** May 11, 2021
Accepted: May 15, 2021
Corresponding author: Yung-Liang Wan, MD, Department of Medical Imaging and Intervention, Linkou Chang Gung Memorial Hospital, College of Medicine, Chang Gung University, No. 5, Fuxing Street, Guishan Dist., Taoyuan 333423, Taiwan.
• E-mail: ylw0518@cgmh.org.tw

functional CT techniques, including static and dynamic CT perfusion (CTP) and CT-derived FFRCT, to assess myocardial ischemia in patients with known or suspected CAD. The current clinical evidence and recent developments in each technique will also be discussed.

Gold Standard of Functional Assessment of CAD

FFR is defined as the ratio of the post-stenotic blood pressure to the pre-stenotic blood pressure in a CAD during maximal hyperemia [9]. FFR can be measured with a pressure wire during ICA to evaluate the hemodynamic significance of stenosis. An FFR value of ≤ 0.80, has excellent diagnostic accuracy (> 90%) for identifying coronary stenosis that causes myocardial ischemia. The landmark FAME (FFR vs. angiography for multivessel evaluation) study [10] revealed that in the FFR-guided percutaneous coronary intervention (PCI) group, drug-eluting stents were deployed at the ischemia-induced lesion with an FFR value of ≤ 0.8. The results revealed favorable clinical outcomes in these patients, as evidenced by a significant decrease in major adverse cardiac events (MACE). Thus, FFR-guided PCI should be the standard protocol for reducing the number of stented arteries and using fewer resources. The series of articles based on the FAME study set up a cornerstone for interventional cardiology. In cases with ambiguous results from nuclear medicine, FFR is mandatory for decision making instead of relying on angiographic findings alone. However, there are well-documented limitations of invasive FFR. For example, FFR may not be reliable in patients with LM or recent myocardial infarction [11]. However, invasive FFR plays an essential role in decision-making and prognostic evaluation. Currently, no studies with large-scale comparisons of invasive and non-invasive assessments of ischemia are available [12]. Interestingly, the results of the recently published ISCHEMIA trial demonstrated no significant difference in reducing cardiovascular events in patients with moderate or severe ischemia between the initial invasive and conservative strategies [13]. This has led to ischemia-driven intervention, which has been the cornerstone of CAD management for decades, and has more recently, become a matter of debate.

CTP for the Heart

Principle of CT Myocardial Perfusion

CTP has been established as a useful imaging tool for functional assessment in patients with ischemic stroke [14]. Compared to other organs, the application of CTP for functional evaluation of heart diseases has been relatively limited, partially because of the technical challenges arising from cardiac motion and beam-hardening artifacts [15]. With the improvement of gantry rotation speed, detector coverage, and image reconstruction algorithms, state-of-the-art clinical CT scanners are capable of performing CT myocardial perfusion imaging robustly to provide incremental diagnostic value to CCTA for a comprehensive anatomic and functional evaluation of CAD in a single cardiac CT test.

CCTA should be performed first as a gatekeeper, and CTP should be acquired as an "add-on" scan to CCTA to detect intermediate lesions. There should be a sufficient wait time (10 minutes or longer) between the CCTA and CTP scans to ensure clearance of contrast and nitroglycerin prior to the CTP scan. Moreover, intravenous administration of a vasodilator, most commonly adenosine and dipyridamole, is necessary for CT myocardial perfusion imaging. More recently, regadenoson has been used as a vasodilator, with a shorter administration time and reduced side effects in patients with asthma or chronic obstructive pulmonary disease [16].

Static CTP

Similar to the assessment of myocardial ischemia with first-pass cardiac magnetic resonance (CMR) and SPECT [17], static CTP assesses the relative distribution of myocardial blood flow (MBF) based on the signal (X-ray attenuation) differences in different regions of the myocardium. Static CTP assesses myocardial perfusion at a single time point during the first pass of contrast in the myocardium [18]. The optimal acquisition time for static CTP is approximately 2 to 10 seconds after the time to peak enhancement of the ascending aorta determined from the test bolus scan, which is acquired prior to the static CTP scan [19]. An illustration of the clinical utility of the static CTP is shown in Figure 1.

Furthermore, both the rest-stress and stress-rest acquisition protocols have been used in clinical static CTP studies. Usually, there is a 10–15 minutes interval between two acquisitions for optimal contrast medium washout [17]. For the rest-stress protocol, the remaining CTP that also provided coronary CTA can be used to exclude patients without coronary artery stenosis and select patients for subsequent stress CTP for the evaluation of myocardial perfusion. The limitation of this protocol is that residual

https://doi.org/10.3348/kjr.2020.1277

Korean Journal of Radiology
KJR

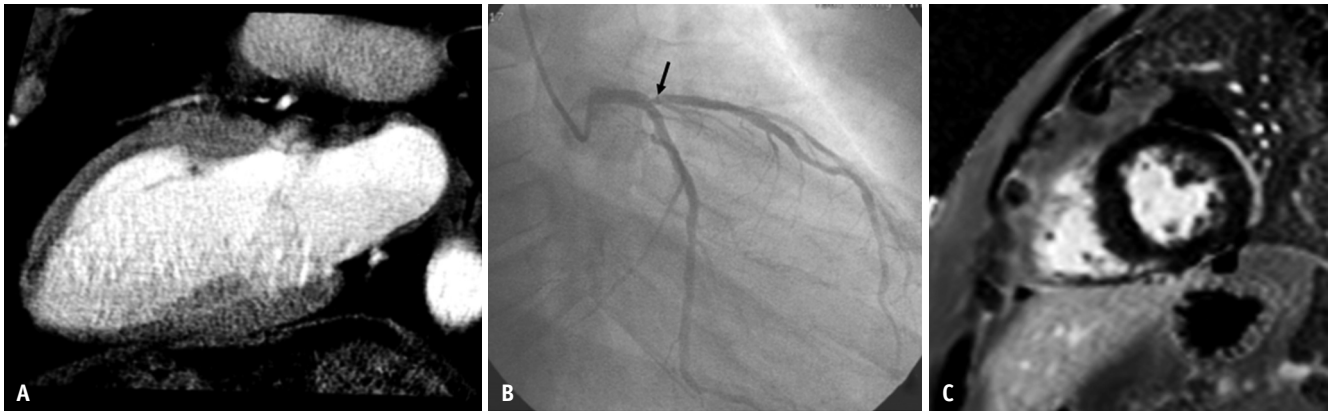

Fig. 1. A 65-year-old male with type 2 diabetes mellitus presented with chest pain.
A. Static CT perfusion assessment from coronary CT angiography source images revealed a non-transmural perfusion defect in the subendocardium in the LAD territory. **B.** The supplying artery LAD had a proximal 70% stenosis (arrow) with an fractional flow reserve value of 0.72, confirming the lesion was functionally significant. **C.** Six months after coronary intervention, the late gadolinium short axis MR image of middle left ventricular wall revealed no myocardial infarction involving the anterior wall. CT = computed tomography, LAD = left anterior descending

contrast medium in the myocardium after rest CTP and the administration of a beta-blocker may affect the assessment of reversible perfusion defects with the subsequent stress CTP. Rest-stress protocol is often used in patients with intermediate coronary stenosis, while the stress-rest protocol is often applied in patients with a high pre-test probability of CAD or post-revascularization status. Stress-rest protocol could avoid the limitation of the rest-stress protocol, but may reduce the sensitivity for the detection of myocardial infarction due to the contamination of the contrast medium from stress CTP masking fixed perfusion defects in the rest CTP [17]. Table 1 shows the radiation dose and diagnostic performance of static and dynamic CTP in comparison with nuclear medicine modalities and invasive FFR.

Diagnostic Performance of Static CTP

The clinical value of static CTP for the functional assessment of CAD has been extensively investigated. To incorporate static CTP into a routine cardiac CT test, a 64-row multidetector CT (MDCT) scanner is the minimal hardware requirement to ensure sufficient temporal and spatial resolution. In 2006, George et al. [20] reported a preclinical study in which myocardial perfusion measurements via static CTP exhibited a good correlation with the reference standard microsphere technique. Before the FAME study, the diagnostic accuracy of static CTP was mainly compared to that of other non-invasive imaging modalities, including positron emission tomography (PET), SPECT, and CMR, as well as ICA. Rocha-Filho et al. [21] reported that the incremental value of static CTP to CCTA with a 64-slice first-generation dual-source CT could improve accuracy from 0.77 to 0.99 by area under the curve (AUC) in detecting significant coronary stenosis. The CORE320, a multicenter study, evaluated the diagnostic performance of static CTP combined with CTA using a wide-detector CT scanner in 381 patients to detect significant coronary stenosis (> 50%) in ICA and myocardial perfusion defects defined by SPECT. In this study, the accuracy of combined static CTP and CTA results in detecting or excluding flow-limiting CAD was 0.87 (95% confidence interval [CI]: 0.84–0.91) [22]. In the sub-analysis of CORE320, when directly comparing static CTP and SPECT, the diagnostic accuracy of MDCT was greater (0.78 vs. 0.69 by AUC) [23].

Compared to the current functional study gold standard, invasive FFR, in a wide-detector CT study with 40 symptomatic patients, Ko et al. [24] reported adding static CTP, including visual assessment and transmural perfusion ratio (TPR) on coronary CTA; as a result, the specificity increased from 78% to 95%, with decreased sensitivity from 95% to 87% and 71%, respectively. In a meta-analysis of 37 studies and 2048 patients in 2015, Takx et al. [25] reported that static CTP, CMR, and PET all had excellent diagnostic accuracy in detecting flow-limiting coronary stenosis (93%, 94%, and 93%, respectively). These diagnostic accuracies were statistically higher than those of traditional modalities, including SPECT myocardial perfusion imaging and stress echocardiography (82% and 83%, respectively). Recently, using a wide-detector CT compared to invasive FFR, Pontone et al. [26] reported static combined CTP and CCTA results with higher diagnostic accuracy than CCTA

 https://doi.org/10.3348/kjr.2020.1277

Table 1. Radiation Dose and Diagnostic Performance of Static and Dynamic CTP in Comparison with Nuclear Medicine Modalities and Invasive FFR

Study	Year	No. (Patient/Vessel)	Technique	Dose (mSv)	Reference	SN (%)	SP (%)	PPV (%)	NPV (%)	Accuracy (%)
SPECT and PET										
Agostini et al. [76]	2018	30	SPECT	8.73 (5.8–13.7)	FFR ≤ 0.8	58	85	37	93	81
			PET	3.1 (2.6–4.2)		67	89	41	95	87
Danad et al. [28]	2017	208/615	SPECT	6.01 ± 0.7	FFR ≤ 0.8	57	94	88	73	77
			PET	3.1		87	84	81	89	85
Static CTP										
Pontone et al. [77] (per-vessel)	2018	88/106	256- slices SSCT (GE)	2.6 ± 1.1	FFR ≤ 0.8	79	97	91	93	92
Bettencourt et al. [78] (per-patient)	2013	101/303	64-slice CT	5 ± 0.96	FFR ≤ 0.8	89 (CTA ≥ 50% and visual perfusion assessment)	83	80	90	85
Wong et al. [27] (per-vessel)	2014	75/127	320- slices SSCT (Toshiba)	4.8	FFR ≤ 0.8	76 (CTA ≥ 50% and visual perfusion assessment)	89	78	88	NA
Ko et al. [24] (per-vessel)	2012	40/118	320- slices SSCT (Toshiba)	4.5 ± 1.8	FFR ≤ 0.8	87 (CTA ≥ 50% and visual perfusion assessment)	95	89	94	92
Dynamic CTP										
Li et al. [43] (per-vessel)	2021	62/95	192-DSCT (Siemens)	3.0	FFR ≤ 0.8	84 (absolute MBF)	98	98	84	91
						96 (MBF ratio)	93	94	95	95
						63 (visual)	98	97	69	79
Yi et al. [47] (per-vessel)	2020	71/174	192-DSCT (Siemens)	3.8 ± 1.4 (low dose CTP: 70 kVp)	FFR ≤ 0.8	78 (absolute MBF)	94	88	88	87
Li et al. [45] (per-vessel)	2019	66/157	192-DSCT (Siemens)	3.6 ± 1.1	FFR ≤ 0.8	96 (absolute MBF)	93	92	96	94
Pontone et al. [42] (per-vessel)	2019	85/255	256- slices SSCT (GE)	5.3 ± 0.7	FFR ≤ 0.8	73 (CCTA + CTP)	86	87	72	82
Coenen et al. [79] (per-vessel)	2017	74	128-slices DSCT (Siemens)	9.3 ± 1.8	FFR ≤ 0.8	73 (index MBF)	68	67	74	70
Rossi et al. [80] (per-vessel)	2017	115	128/192-DSCT (Siemens)	6.0 ± 10.3	FFR ≤ 0.8	89 (relative MBF)	73	67	92	
Kono et al. [81] (per-vessel)	2014	42	128-DSCT (Siemens)	9.4	FFR ≤ 0.8	98 (MBF ratio)	70	76	97	86
Greif et al. [82] (per-vessel)	2013	65/195	128-slices DSCT (Siemens)	9.7 ± 2.2	FFR ≤ 0.8	95 (absolute MBF)	74	98	49	78

CT = computed tomography, CCTA = coronary computed tomography angiography, CTA = computed tomography angiography, CTP = computed tomography perfusion, DSCT = dual source computed tomography, FFR = fractional flow reserve, MBF = myocardial blood flow, NPV = negative predictive value, PET = positron emission tomography, PPV = positive predictive value, SN = sensitivity, SP = specificity, SPECT = single-photon emission computed tomography, SSCT = single source computed tomography

Korean Journal of Radiology
KJR

alone per-vessel (93% vs. 83%) and per patient (91% vs. 76%) in intermediate-to-high-risk symptomatic patients. Semi-quantitative analysis, including the myocardial perfusion reserve index, transluminal attenuation gradient (TAG), and TPR, can also be applied to static CTP. A wide-detector CT study with 75 patients and 44 FFR significant vessels revealed that CTA + TAG had comparable per-vessel diagnostic accuracy to CTA + static CTP with AUC of 0.844 and 0.845, respectively, (p = 0.98). Moreover, combined CTA, CTP, and TAG (AUC = 0.91) had superior diagnostic accuracy to CTA + TAG and CTP + CTA (p = 0.01) [27].

Limitation and Recent Developments of Static CTP

Static CTP based on the regular coronary CTA protocol may not acquire myocardial imaging at the optimal timing of the time-attenuation curve (TAC) with peak enhancement in only one single-phase acquisition during the first pass of the contrast medium [17]. This could lead to an underestimation of the perfusion defects. In addition, single-phase images cannot generate quantitative (absolute) MBF and blood volume maps. Artifacts related to beam hardening, breath, and high heart rate may also impose a burden on diagnostic accuracy [15].

State-of-the-art clinical CT scanners developed by major vendors are equipped with dual-energy imaging capabilities. For instance, a dual-source or dual-layer CT scanner enables the differentiation of materials with similar attenuation coefficients but different atomic numbers. By simultaneously acquiring an additional scan with a different X-ray energy spectrum, additional spectral information may allow better differentiation of tissues with similar X-ray attenuation properties at a specific X-ray energy level [28].

Moreover, in dual-energy CT, the virtual monoenergetic images generated by blending the high- and low-energy scan data for the optimal signal-to-noise ratio could reduce beam-hardening artifacts [29]. In addition, both iodine analysis (quantitative) and eyeball (qualitative) analysis can be achieved by operating a static CTP. With regard to the radiation issue, by advanced iterative reconstruction, the radiation dose of DECT is not higher than the single energy mode in dual-source CT [30]. A dual-layer detector CT system automatically generates iodine maps and virtual monoenergetic images in static CTP study. Carrascosa et al. [31] reported that the diagnostic performance of dual-energy static CTP was greater than that of single-energy static CTP in identifying perfusion defects (AUC: 0.90 [0.86–0.94] vs. 0.80 [0.76–0.84], respectively; p < 0.005) and remained unaffected when including only segments affected by beam-hardening artifacts (AUC: 0.90 [0.84–0.96] vs. 0.77 [0.69–0.84]; p = 0.007). The accuracy of iodine concentration analysis of both dual-energy and dual-layer CT systems has been validated in a phantom study [32]. A study comparing CMR and an iodine map generated from dual-energy static CTP demonstrated differences in the iodine concentration of the myocardium (p < 0.001) among normal (2.56 ± 0.66 mg/mL), ischemic (1.98 ± 0.36 mg/dL), and infarcted segments (1.35 ± 0.57 mg/mL) [33]. The optimal myocardial iodine concentration threshold to differentiate between normal and pathologic myocardium was 2.1 mg/mL (sensitivity 75%, specificity 73.6%, ROC curve 0.806, and reproducibility of 0.814 [intraclass correlation coefficient]). However, some shared limitations in stress CTP are still present in DECT, including the impact of high heart rate during adenosine infusion on imaging quality and inaccurate iodine concentration measurements of the myocardium with motion artifacts.

Dynamic CTP

The technological requirement of a dynamic CTP is higher than that of a static CTP. Specifically, the entire left ventricle of the heart should be covered in one or two scanner table positions in a non-helical/non-spiral acquisition mode. This restricts dynamic CTP to the latest generation of wide-detector CT and 2nd/3rd-generation dual-source CT owing to its higher temporal resolution and wider coverage. In approximately 30 seconds, a continuous scan of the left ventricle can be performed to acquire the image dataset of the first-pass contrast medium through the left ventricle cavity, aorta, and myocardial microcirculation. The end-systolic phase is preferred over the prospective electrocardiography-gated acquisition protocol for dynamic CTP as this can reduce beam hardening and motion artifacts [34]. With the CT attenuation changes in serial images of the myocardium and aorta, the software can generate the TAC and calculate the MBF and myocardial blood volume by dividing the convoluted maximal slope of the myocardial TAC by the maximum arterial input function [35]. Color-coded volumetric maps, polar maps, or bull's eye plots can be generated for the diagnosis of myocardial ischemia. In addition to quantitative analysis, another advantage of dynamic CTP over static CTP is the detection of balanced ischemia in patients with multivessel disease and in diabetic patients with microvascular disease, which may be

 https://doi.org/10.3348/kjr.2020.1277

missed in qualitative analysis by static CTP [36].

To combine with CCTA, theoretically, dynamic CTP should be performed before CCTA to avoid the presence of residual contrast medium in the myocardium and facilitate an optimal CTP map. However, in a clinical scenario, CCTA selected patients with intermediate and high-grade coronary stenosis for subsequent functional assessment, which avoids unnecessary radiation exposure and contrast medium administration in patients without obstructive CAD. Therefore, for suspected CAD patients, the workflow should involve immediate interpretation of CCTA, which also provides the time window for myocardial contrast medium washout. Moreover, the cardiac imager should be the key person who decides to perform dynamic CTP for the patient [37].

Diagnostic Performance of Dynamic CTP

In animal studies, MBF assessed by CTP has a good correlation with FFR and MBF assessed by microspheres [38,39]. Since 2011, multiple clinical studies have demonstrated a good correlation between dynamic CTP and directly measured invasive FFR [35,40,41]; as a result, the diagnostic accuracy of dynamic CTP has become increasingly accepted. Bamberg et al. [40] compared dynamic CTP using 2nd-generation dual-source CT and invasive FFR and showed that CT-derived MBF reclassified coronary lesions depicted by CCTA with significantly improved PPV (49% to 78% [95% CI: 61%, 89%; $p = 0.02$]). In a meta-analysis study in 2015, Takx et al. [25] reported that diagnostic accuracy was similar among dynamic CT (AUC, 0.93), MRI (AUC, 0.94), and PET (AUC, 0.93), and lower in SPECT (AUC, 0.83) and stress echocardiography (AUC, 0.82).

More recently, Pontone et al. [42] reported that the diagnostic performance of dynamic CTP was comparable to that of invasive FFR, with a sensitivity of 73%, specificity of 86%, and accuracy of 0.88. However, the cut-off values of CT-derived MBF for hemodynamic significance vary between 75 and 164 mL/min/g among studies; such discrepancies could be related to different acquisition protocols employed for dynamic CTP assessment, CT technology, and pathologic conditions such as collateral circulation [35,40,41]. This had a great influence on the diagnostic accuracy of dynamic CTP and greatly improved the accuracy of dynamic CTP to facilitate its clinical implementation for the functional assessment of CAD. A dynamic CTP study can provide visual and quantitative assessments. Li et al. [43] conducted a direct comparison of both methods in detecting functionally significant coronary stenosis, and revealed that MBF is superior to visual analysis at the per-lesion level (AUC = 0.942, 0.802, $p < 0.01$) in 62 patients with 95 target vessels.

Limitation and Recent Developments of Dynamic CTP

In the past, the radiation exposure of dynamic CTP was much higher than that of static CTP [44]. Nowadays, dynamic CT study using an advanced CT scanner have a similar radiation dose (mean 3.6 mSv) to that of static CTP study [45]. Table 2 shows a direct comparison of the clinical value in static and dynamic CTP, as well as the technique.

In clinical practice, beam-hardening artifacts arising from dense iodinated contrast medium in the aorta and heart chamber pose a challenge to the accurate assessment of MBF in dynamic CTP [15]. DECT is capable of virtually synthesizing monoenergetic images and reducing beam-hardening artifacts [26]. In a pig dynamic perfusion study

Table 2. Comparison between Static vs. Dynamic CTP

	Static CTP	Dynamic CTP
Scanner	All CT scanners with ≥ 64 slices	Wide-detector (whole heart coverage) and the 2nd/3rd generation dual source CT
Scan protocol	The same as single phase CTA. To start the scan 2–10 seconds away from the peak enhancement of ascending aorta	Repeated acquisition during the first-pass contrast medium of left ventricle and myocardium for generating time-attenuation curve
Breath holding time	Less than 10 seconds	About 30 seconds
Radiation dose	2–9 mSv (rest and stress)	3.6 mSv (stress only in the 3rd generation dual source CT)
Beam-hardening artifacts	Yes	Yes
Post processing by software	Less	Yes
Imaging interpretation	Visual (mainly) and semi-quantitative like TPR, MPRI	Quantitation of myocardial blood flow and volume

CT = computed tomography, CTP = computed tomography perfusion, CTA = computed tomography angiography, MPRI = myocardial perfusion reserve index, TPR = transmural perfusion ratio

https://doi.org/10.3348/kjr.2020.1277

Korean Journal of Radiology
KJR

with a prototypic dual-layer CT system, Fahmi et al. [46] reported that virtual monoenergetic images could be used to improve the over-estimation of functional severity on the ischemic anterior wall. In this study, the functional severity was due to beam-hardening artifact-induced hypoenhancement, and was assessed by the "endo-to-epi" transmural flow ratio for subendocardial ischemia in images of 120 kVp vs 70 keV. (0.29 ± 0.01 vs. 0.55 ± 0.01; $p < 0.05$). Furthermore, the potential incremental value of coronary CTA extracted from the stress-dynamic CTP has also been investigated. Yi et al. [47] reported that CTP-derived single-phase CTA improved the diagnostic value compared to CTP alone (AUC: 0.963 vs. 0.922; $p < 0.01$) using a 3rd-generation dual-source CT. Additionally, the study team used a 70-kVp stress CTP protocol. It is possible to further reduce the radiation dose and total scan time for a real "one-stop shop" study of CAD using an advanced CT machine for future clinical practice.

FFRCT

Principle of FFRCT

Without direct invasive measurement, by applying computational fluid dynamics, FFRCT can perform the simultaneous calculation of pressure and flow along coronary arteries from CCTA data [48]. There are several essential principles and steps to acquire "virtual" FFR non-invasively: 1) the total coronary flow meets the myocardial demand in a state of rest, which can be calculated from the ventricular volume and mass using an anatomical model, 2) coronary microvascular resistance of the myocardium is inversely related to the epicardial coronary arteries, 3) the response of the vasodilator of coronary arteries is predictable and can be used to simulate the reduction in microvascular resistance during maximal hyperemia from images acquired at rest, and 4) the flow and pressure along the coronary vascular bed can be computed by solving the three-dimensional Navier–Stokes equation, which comprises a set of nonlinear partial differential equations (Fig. 2) [49].

To date, there have been several companies, including HeartFlow®, Siemens, Canon, KEYAMEDICAL®, AI Medic®, United Imaging Healthcare, and the EU-funded Horizon 2020 project SMARTool, that have used the computed fluid dynamics (CFD) technique in FFRCT. HeartFlow® FFRCT is currently the most popular in the United States, Europe, and Japan, and is the only technique approved by the American Food and Drug Administration. For hospitals that have a contract with HeartFlow®, the CCTA data have to be transferred to the core laboratory of HeartFlow (Redwood, CA, USA) for subsequent processing, which takes between 1 and 4 hours. A clinical example illustrating the utility of FFRCT from HeartFlow is presented in Figure 3.

All other CFD-based techniques, including cFFR (combined CFD-based method and machine learning [ML]) (Siemens), 1-D CFD (Canon Medical Systems Corporation), uCT-FFR (United-Imaging Healthcare), AI Medic® (HeartMedi), reduced-order model FFRCT (Comprehensive Cardiac Analysis, IntelliSpace, Philips Healthcare), and DEEPVESSEL FFR (combined CFD-based method and deep learning) (Keya Medical Technology), can be used "on-site." Moreover, the computer hardware requirements of these types of software are significantly less complex, and the entire process can be completed within 10 to 30 minutes [50-54]. It is worth mentioning that AI Medic® (HeartMedi) has been

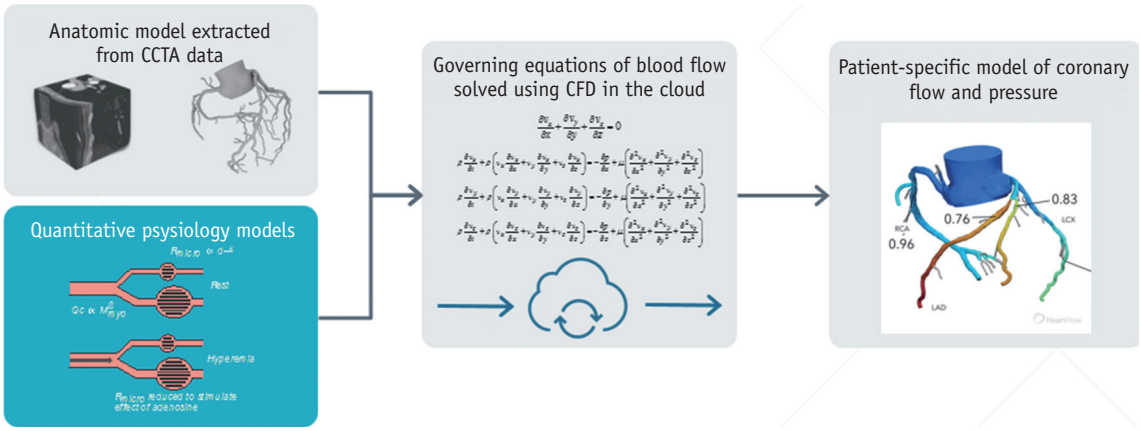

Fig. 2. The HeartFlow process demonstrates the CFD applied to cardiac computed tomography for noninvasive quantification of fractional flow reserve. CCTA = coronary computed tomography angiography, CFD = computed fluid dynamics

https://doi.org/10.3348/kjr.2020.1277

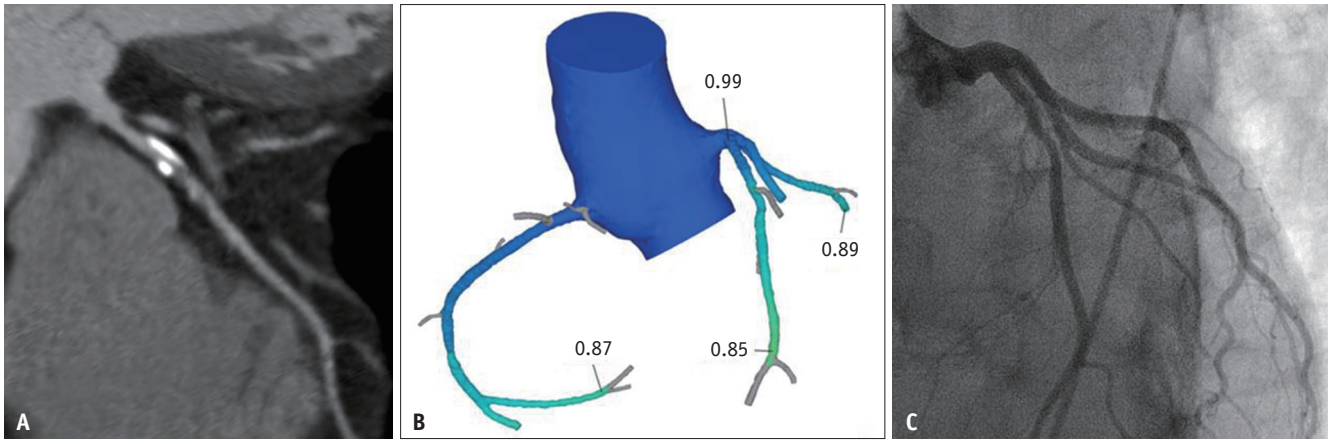

Fig. 3. A 45-year-old female without any coronary artery disease risk factors presented with dyspnea and chest tightness.
A-C. Reformatted coronary computed tomography angiograms **(A)** and non-invasive fractional flow reserve assessment **(B)** of the left anterior descending artery in comparison with the corresponding invasive coronary angiographic image **(C)**.

approved by the National Institute of Medical Device Safety Information and is currently in the final stage of clinical trials in South Korea [53]. Currently, most other techniques are used only for research purposes. Table 3 shows the diagnostic performance of FFRCT from different software companies in comparison with the invasive FFR.

Recently, the Radiological Society of North America issued recommendations for FFRCT for the interpretation and reporting of physicians. FFRCT values of > 0.80 are considered normal, indicating myocardium supply by vessels distal to the stenosis rarely under ischemic status, while values of ≤ 0.75, are considered as lesion-specific ischemia. In coronary lesions with FFRCT values between 0.76 and 0.80, additional risk stratification is recommended. This is particularly crucial because the values assessed by FFRCT are slightly lower than those of invasive FFR [55,56], although this has been considered a "gray area" in the invasive measurements. In addition, for patients with negative results or non-obstructive lesions (< 50% stenosis) of CCTA, no further FFRCT is needed. FFRCT can be useful in anatomically moderate (50%–69%) and severe (70%–99%) stenosis [57].

Diagnostic Performance of FFRCT

The diagnostic performance of FFRCT has been validated in several major studies, predominantly using the HeartFlow® technique [48,55,56,58,59]. Promising data from three major studies, including DISCOVER-FLOW, DeFACTO, and HeartFlow NXT, demonstrated that using FFRCT < 0.8 as the cutoff value for lesion-specific ischemia shows a good correlation between FFRCT and invasive FFR. In the DISCOVER-FLOW study, the results of FFRCT of 158 vessels from 103 patients showed a per-vessel sensitivity of 87.9%, a specificity of 82.2%, and an accuracy of 84.3% compared to invasive FFR. The ROC curve for detecting a functionally significant lesion defined by invasive FFR (FFR < 0.80) was significantly improved in FFRCT compared to standard CCTA (0.90 vs. 0.75, $p = 0.001$) [49]. In two subsequent large studies (DeFACTO and NXT), the investigators demonstrated the incremental diagnostic value of FFRCT over CCTA in detecting functionally significant stenosis defined by invasive FFR [60], as well as a good correlation between FFRCT and invasive FFR (Pearson's R = 0.82; $p < 0.001$) [55]. The CFD-based SmartFFR from SMARTool showed a fast processing time (25 ± 10 minutes) and a strong correlation with invasive FFR (R = 0.93, $p < 0.001$) [59]. In contrast, in a single-center, prospective study of 63 patients, the deep-learning-based method, DEEPVESSEL FFR, showed good correlation with invasive FFR (R = 0.686, $p < 0.001$), with a per-vessel sensitivity of 97.1%, specificity of 75%, and accuracy of 87.3% for detecting invasive FFR < 0.8 [54].

The diagnostic accuracy of FFRCT in patients with heavy calcified coronary burden is another important issue. In a sub-study of an NXT trial, Nørgaard et al. [61] showed no significant differences in FFRCT in detecting ischemia between moderate-high Agatston scores (121–1703) and low-mild scores (0–120). However, two studies using ML FFRCT (cFFR) showed contrasting results. Tesche et al. [62] reported that FFRCT had superior diagnostic value to CTA in vessels with high Agatston scores (> 400) (AUC: 0.71, 0.55, $p = 0.04$), good discriminatory power in vessels with high Agatston scores (> 400), and high performance in

https://doi.org/10.3348/kjr.2020.1277

Table 3. Diagnostic Performance of FFRCT in Comparison with Invasive FFR

Study	Year	No. (Patient/Vessels)	Software	Reference	SN (%)	SP (%)	PPV (%)	NPV (%)	Accuracy (%)	CTA Accuracy (%)
Tang et al. [51]	2020	338/422	uCT-FFR version 1.5 on-site CFD-based model	FFR ≤ 0.8 (per-vessel)	89	91	86	94	91	55
Wang et al. [54]	2019	63/71	DEEPVESSEL FFR@ online CFD-DL-based model	FFR ≤ 0.8 (per-vessel)	97	75	83	96	87	NA
Li et al. [45]	2019	86/157	cFFR (version 3.0, Siemens)	FFR ≤ 0.8 (per-vessel)	88	68	72	86	78	0.72
Siogkas et al. [59]	2019	63/74	vFAI SMARTool	FFR ≤ 0.8 (per-vessel)	88	96	91	94	93	NA
Coenen et al. [83] (MACHINE consortium)	2018	351/525	ML- vs. CFD based cFFR (version 3.0, Siemens)	FFR ≤ 0.8 (per-vessel)	ML 81 CFD 82	76 76	70 70	85 86	78 78	66
Ko et al. [84]	2017	42/78	1-D CFD (Canon Medical Systems Corporation)	FFR ≤ 0.8 (per-vessel)	78	87	74	89	84	69
Chung et al. [85] (NOVEL-FLOW)	2017	117/218	3D-CFD with lumped parameter mode	FFR ≤ 0.8 (per-vessel)	86	86	80	90	86	66
Coenen [50]	2015	106	cFFR (version 1.4, Siemens)	FFR ≤ 0.8 (per-vessel)	88	65	65	88	75	56
Nørgaard et al. [61] (NXT trial)	2015	251/484	FFR-CT off-site CFD-based model (HeartFlow)	FFR ≤ 0.8 (per-vessel)	84	86	61	95	86	65
Min et al. [66] (DeFACTO trial)	2012	252/407	FFR-CT off-site CFD-based model (HeartFlow)	FFR ≤ 0.8 (per-patient)	90	54	67	95	73	64
Koo et al. [49] (DISCOER-Flow trial)	2011	159/103	FFR-CT (HeartFlow)	FFR ≤ 0.8 (per-vessel)	88	82	74	92	84	59

CFD = computational fluid dynamic, CT = computed tomography, CTA = computed tomography angiography, DL = deep learning, FFR = fractional flow reserve, ML = machine learning, NPV = negative predictive value, PPV = positive predictive value, SN = sensitivity, SP = specificity

https://doi.org/10.3348/kjr.2020.1277

Korean Journal of Radiology KJR

low-to-intermediate Agatston scores (0 to 400), with a statistically significant difference (AUC: 0.71 vs. 0.85, $p = 0.04$). Moreover, in a Chinese multicenter study, there was no statistical difference in the diagnostic accuracy, sensitivity, or specificity of FFRCT across different calcified plaque patterns and Agaston score levels [63]. The different conclusions of these two studies is probably attributed to different study populations with various calcified burdens and different versions of cFFR (2.1% vs. 3.1%). In addition, Tang et al. [51] demonstrated no significant difference in the diagnostic performance of the other ML FFRCT (uCT-FFR) between patients with calcium scores of ≥ 400 and < 400 ($p = 0.393$).

Direct Comparison between CTP and FFRCT

Recently, many researchers have focused on the integration and comparison of different methodologies of cardiac CT, including static and dynamic CTP, CTA, and FFRCT, in the diagnosis of ischemic-specific CAD. Pontone et al. [42] reported that integrated CTA, FFRCT, and dynamic-stress CTP performed by a whole-heart cover CT scanner in 85 symptomatic, intermediate to high-risk patients, integrated CTA, CTP, and FFRCT outperformed other methods in detecting functionally significant CAD (CTA + CTP + FFRCT: AUC: 0.919, CTA + FFRCT: 0.878, CTA + CTP: 0.876, CTA: 0.826). In the PERFECTION study, which performed a direct comparison of FFRCT, static CTP, and invasive FFR in 147 symptomatic patients, both static CTP and FFRCT were found to perform better than CTA alone per patient (accuracies of 92% and 94% vs. 82%, respectively, both $p < 0.001$). There was no significant difference between FFRCT + CCTA and static CTP + CCTA [64].

More recent studies have used other FFRCT techniques. In an ML-based FFRCT (cFFR) study with 86 subjects and 157 target vessels, dynamic CT MPI outperformed cFFR for the diagnosis of functionally significant coronary stenosis (diagnostic accuracy: 84% vs. 78%, $p = 0.04$) [45]. Traditionally, anatomical intermediate lesions of coronary CTA require further tests to detect functionally significant diseases. Several studies, including on- and off-site FFRCT software techniques, have been discussed in relation to this issue. In the NXT trial, subsequent analyses were restricted to patients with intermediate stenoses ranging from 30% to 70% (n = 235), with sensitivity, specificity, positive predictive value, negative predictive value, and accuracy of 85%, 79%, 63%, 92%, and 80%, respectively [55]. In other off-site CFD-based FFRCT studies, on a per-vessel basis, the AUCs were 0.79 and 0.95 with 150 lesions in 82 patients [65] and 66 vessels in 60 patients [66], respectively, and 0.86 in the reduced-order model FFRCT

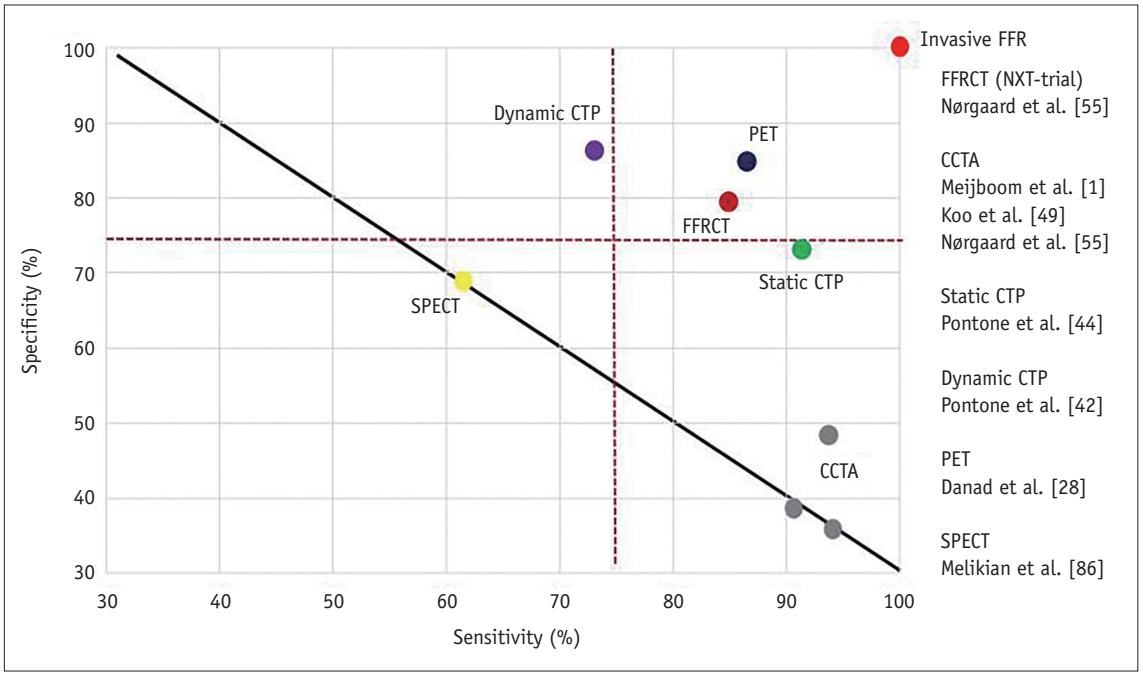

Fig. 4. Specificity versus sensitivity plots of different imaging modalities for assessment of functional coronary artery disease.
The figures in parentheses refer to the reference numbers. CCTA = coronary computed tomography angiography, CT = computed tomography, CTP = computed tomography perfusion, FFR = fractional flow reserve, PET = positron emission tomography, SPECT = single-photon emission computed tomography

https://doi.org/10.3348/kjr.2020.1277

Korean Journal of Radiology
KJR

with 60 lesions in 66 patients [67]. In addition, in a dynamic CTP and FFRCT study, the per-vessel sensitivity and specificity of FFRCT for intermediate stenosis (30%–60%) was 100% and 50%, respectively, which led to a large proportion of false positive lesions of FFRCT [45]. Moreover, the diagnostic performance of dynamic CTP was much better than that of FFRCT (AUC: 0.99 vs. 0.77). However, in a recent study on 246 patients, one on-site FFRCT (uCT-FFR) demonstrated an AUC of 0.94 (95% CI: 0.90 to 0.97) on a per-vessel basis in 299 vessels with intermediate stenosis [51]. It is predictable that different diagnostic performances could be related to various algorithms in different study populations. Figure 4 shows the results of selected studies evaluating the diagnostic performance of static, dynamic CTP, FFRCT, and other non-invasive modalities compared to invasive FFR, the gold standard of the functional study of CAD.

In terms of prognostic value, in a dynamic CTP study with 332 patients with suspected CAD, abnormal perfusion was an independent predictor (hazard ratio: 5.7, 95% CI: 1.9–16.9, $p = 0.002$) of MACE, with a significant improvement in prognostic value during a median follow-up of 2.5 years [68]. In the CORE320 study, the prognostic value of the identification of MACE at the 2-year follow-up was similar ($p = 0.36$) for combined static CTP and CTA (AUC: 0.68; 95% CI: 62–75), and for ICA and SPECT (AUC: 0.71; 95% CI: 65–79) [69]. In a clinical utility trial, the PLATFORM study demonstrated a low adverse event rate (5 of 581 followed-up cases) in the group cared for by the FFRCT guide [70]. Another prospective multicenter registry, the ADVANCE study, enrolled 5083 patients with stable angina and showed that FFRCT increased the number of subjects referred to ICA. Moreover, patients with FFRCT < 0.8, were more likely to have anatomical significant CAD and had a much higher MACE at 90 days of follow-up [57].

Limitations and Recent Developments of FFRCT

The rejection rate of FFRCT is relatively high. Indeed, in the ADVANCE registry and a large cohort study, the rejection rates of FFRCT were 2.9% and 8.4%, respectively [71], with responsible factors including calcified blooming, inadequate contrast enhancement, image noise, misalignment, and metal artifacts [62]. Excellent image quality of CCTA is needed to avoid these artifacts for robust FFRCT analysis. In addition, FFRCT cannot be used in patients with coronary occlusion associated with collateral circulation, because such a complicated condition cannot be handled by the current FFRCT analytic algorithm [55]. Both off-site FFRCT (HeartFlow) and various on-site technologies require accurate delineation of the boundaries of coronary artery trees for subsequent fluid analysis [72]. Most commercialized software is semi-automatic and requires manual correction, especially for vessels with a heavy calcified burden [72-74]. Recently, Kumamaru et al. [75] reported a 3D deep-learning-based software that could fully and automatically analyze unsegmented coronary CTA data. However, as this was a retrospective study with a small sample size, future work is needed to fully and automatically analyze FFRCT to reduce time and avoid inter- and intra-observer variabilities.

Summary

Recently, due to improved CT scanners and technologies, cardiac CT can provide functional information using FFRCT and CTP. Combined with CCTA, cardiac CT is the only modality that can provide a “one-stop shop” service. Compared to static CTP, which is mainly observed by eye, dynamic CTP requires software to generate MBF for full quantitative assessment. Although FFRCT requires no additional scan, “on-site” or “off-site” post-processing software is required to generate the results. Based on clinical data and CCTA, radiologists should choose adequate techniques to provide valuable functional information for clinicians.

Conflicts of Interest

The authors have no potential conflicts of interest to disclose.

Author Contributions

Conceptualization: Chun-Ho Yun, Yung-Liang Wan. Methodology: Chun-Ho Yun, Chung-Lieh Hung, Ming-Shien Wen. Project administration: Yung-Liang Wan. Resources: Chun-Ho Yun, Yung-Liang Wan. Supervision: Yung-Liang Wan. Validation: Aaron So. Visualization: Chun-Ho Yun, Aaron So. Writing—original draft: Chun-Ho Yun. Writing—review & editing: all authors.

ORCID iDs

Chun-Ho Yun
https://orcid.org/0000-0002-2463-1726
Chung-Lieh Hung
https://orcid.org/0000-0002-2858-3493
Ming-Shien Wen
https://orcid.org/0000-0002-0056-7985

 https://doi.org/10.3348/kjr.2020.1277

Yung-Liang Wan
https://orcid.org/0000-0002-3039-996X
Aaron So
https://orcid.org/0000-0001-9293-158X

REFERENCES

1. Meijboom WB, Meijs MF, Schuijf JD, Cramer MJ, Mollet NR, van Mieghem CA, et al. Diagnostic accuracy of 64-slice computed tomography coronary angiography: a prospective, multicenter, multivendor study. *J Am Coll Cardiol* 2008;52:2135-2144
2. Budoff MJ, Dowe D, Jollis JG, Gitter M, Sutherland J, Halamert E, et al. Diagnostic performance of 64-multidetector row coronary computed tomographic angiography for evaluation of coronary artery stenosis in individuals without known coronary artery disease: results from the prospective multicenter ACCURACY (Assessment by Coronary Computed Tomographic Angiography of Individuals Undergoing Invasive Coronary Angiography) trial. *J Am Coll Cardiol* 2008;52:1724-1732
3. Nikolaou K, Knez A, Rist C, Wintersperger BJ, Leber A, Johnson T, et al. Accuracy of 64-MDCT in the diagnosis of ischemic heart disease. *AJR Am J Roentgenol* 2006;187:111-117
4. Miller JM, Rochitte CE, Dewey M, Arbab-Zadeh A, Niinuma H, Gottlieb I, et al. Diagnostic performance of coronary angiography by 64-row CT. *N Engl J Med* 2008;359:2324-2336
5. Smith SC Jr, Feldman TE, Hirshfeld JW Jr, Jacobs AK, Kern MJ, King SB 3rd, et al. ACC/AHA/SCAI 2005 guideline update for percutaneous coronary intervention: a report of the American College of Cardiology/American Heart Association Task Force on Practice Guidelines (ACC/AHA/SCAI Writing Committee to Update 2001 Guidelines for Percutaneous Coronary Intervention). *Circulation* 2006;113:e166-e286
6. Patel MR, Dehmer GJ, Hirshfeld JW, Smith PK, Spertus JA. ACCF/SCAI/STS/AATS/AHA/ASNC 2009 appropriateness criteria for coronary revascularization: a report by the American College of Cardiology Foundation Appropriateness Criteria Task Force, Society for Cardiovascular Angiography and Interventions, Society of Thoracic Surgeons, American Association for Thoracic Surgery, American Heart Association, and the American Society of Nuclear Cardiology Endorsed by the American Society of Echocardiography, the Heart Failure Society of America, and the Society of Cardiovascular Computed Tomography. *J Am Coll Cardiol* 2009;53:530-553
7. Patel MR, Calhoon JH, Dehmer GJ, Grantham JA, Maddox TM, Maron DJ, et al. ACC/AATS/AHA/ASE/ASNC/SCAI/SCCT/STS 2016 appropriate use criteria for coronary revascularization in patients with acute coronary syndromes : a report of the American College of Cardiology Appropriate Use Criteria Task Force, American Association for Thoracic Surgery, American Heart Association, American Society of Echocardiography, American Society of Nuclear Cardiology, Society for Cardiovascular Angiography and Interventions, Society of Cardiovascular Computed Tomography, and the Society of Thoracic Surgeons. *J Nucl Cardiol* 2017;24:439-463
8. Neumann FJ, Hochholzer W, Siepe M. ESC/EACTS guidelines on myocardial revascularization 2018 : the most important innovations. *Herz* 2018;43:689-694
9. Pijls NH, De Bruyne B, Peels K, Van Der Voort PH, Bonnier HJ, Bartunek J, et al. Measurement of fractional flow reserve to assess the functional severity of coronary-artery stenoses. *N Engl J Med* 1996;334:1703-1708
10. Tonino PA, De Bruyne B, Pijls NH, Siebert U, Ikeno F, van' t Veer M, et al. Fractional flow reserve versus angiography for guiding percutaneous coronary intervention. *N Engl J Med* 2009;360:213-224
11. Pijls NH, Tanaka N, Fearon WF. Functional assessment of coronary stenoses: can we live without it? *Eur Heart J* 2013;34:1335-1344
12. Plein S, Motwani M. Fractional flow reserve as the reference standard for myocardial perfusion studies: fool's gold? *Eur Heart J Cardiovasc Imaging* 2013;14:1211-1213
13. Maron DJ, Hochman JS, Reynolds HR, Bangalore S, O'Brien SM, Boden WE, et al. Initial invasive or conservative strategy for stable coronary disease. *N Engl J Med* 2020;382:1395-1407
14. Wintermark M, Albers GW, Alexandrov AV, Alger JR, Bammer R, Baron JC, et al. Acute stroke imaging research roadmap. *Stroke* 2008;39:1621-1628
15. Mushtaq S, Conte E, Pontone G, Baggiano A, Annoni A, Formenti A, et al. State-of-the-art-myocardial perfusion stress testing: static CT perfusion. *J Cardiovasc Comput Tomogr* 2020;14:294-302
16. Seitun S, Castiglione Morelli M, Budaj I, Boccalini S, Galletto Pregliasco A, Valbusa A, et al. Stress computed tomography myocardial perfusion imaging: a new topic in cardiology. *Rev Esp Cardiol (Engl Ed)* 2016;69:188-200
17. Sørgaard MH, Linde JJ, Kühl JT, Kelbæk H, Hove JD, Fornitz GG, et al. Value of myocardial perfusion assessment with coronary computed tomography angiography in patients with recent acute-onset chest pain. *JACC Cardiovasc Imaging* 2018;11:1611-1621
18. Kurata A, Mochizuki T, Koyama Y, Haraikawa T, Suzuki J, Shigematsu Y, et al. Myocardial perfusion imaging using adenosine triphosphate stress multi-slice spiral computed tomography: alternative to stress myocardial perfusion scintigraphy. *Circ J* 2005;69:550-557
19. Bischoff B, Bamberg F, Marcus R, Schwarz F, Becker HC, Becker A, et al. Optimal timing for first-pass stress CT myocardial perfusion imaging. *Int J Cardiovasc Imaging* 2013;29:435-442
20. George RT, Silva C, Cordeiro MA, DiPaula A, Thompson DR, McCarthy WF, et al. Multidetector computed tomography myocardial perfusion imaging during adenosine stress. *J Am Coll Cardiol* 2006;48:153-160
21. Rocha-Filho JA, Blankstein R, Shturman LD, Bezerra HG, Okada DR, Rogers IS, et al. Incremental value of adenosine-induced stress myocardial perfusion imaging with dual-source

https://doi.org/10.3348/kjr.2020.1277

CT at cardiac CT angiography. *Radiology* 2010;254:410-419
22. Rochitte CE, George RT, Chen MY, Arbab-Zadeh A, Dewey M, Miller JM, et al. Computed tomography angiography and perfusion to assess coronary artery stenosis causing perfusion defects by single photon emission computed tomography: the CORE320 study. *Eur Heart J* 2014;35:1120-1130
23. George RT, Mehra VC, Chen MY, Kitagawa K, Arbab-Zadeh A, Miller JM, et al. Myocardial CT perfusion imaging and SPECT for the diagnosis of coronary artery disease: a head-to-head comparison from the CORE320 multicenter diagnostic performance study. *Radiology* 2014;272:407-416
24. Ko BS, Cameron JD, Leung M, Meredith IT, Leong DP, Antonis PR, et al. Combined CT coronary angiography and stress myocardial perfusion imaging for hemodynamically significant stenoses in patients with suspected coronary artery disease: a comparison with fractional flow reserve. *JACC Cardiovasc Imaging* 2012;5:1097-1111
25. Takx RA, Blomberg BA, El Aidi H, Habets J, de Jong PA, Nagel E, et al. Diagnostic accuracy of stress myocardial perfusion imaging compared to invasive coronary angiography with fractional flow reserve meta-analysis. *Circ Cardiovasc Imaging* 2015;8:e002666
26. Pontone G, Andreini D, Guaricci AI, Baggiano A, Fazzari F, Guglielmo M, et al. Incremental diagnostic value of stress computed tomography myocardial perfusion with whole-heart coverage CT scanner in intermediate-to high-risk symptomatic patients suspected of coronary artery disease. *JACC Cardiovasc Imaging* 2019;12:338-349
27. Wong DT, Ko BS, Cameron JD, Leong DP, Leung MC, Malaiapan Y, et al. Comparison of diagnostic accuracy of combined assessment using adenosine stress computed tomography perfusion + computed tomography angiography with transluminal attenuation gradient + computed tomography angiography against invasive fractional flow reserve. *J Am Coll Cardiol* 2014;63:1904-1912
28. Danad I, Raijmakers PG, Driessen RS, Leipsic J, Raju R, Naoum C, et al. Comparison of coronary CT angiography, SPECT, PET, and hybrid imaging for diagnosis of ischemic heart disease determined by fractional flow reserve. *JAMA Cardiol* 2017;2:1100-1107
29. Vliegenthart R, Pelgrim GJ, Ebersberger U, Rowe GW, Oudkerk M, Schoepf UJ. Dual-energy CT of the heart. *AJR Am J Roentgenol* 2012;199:S54-S63
30. Cademartiri F, Seitun S, Clemente A, La Grutta L, Toia P, Runza G, et al. Myocardial blood flow quantification for evaluation of coronary artery disease by computed tomography. *Cardiovasc Diagn Ther* 2017;7:129-150
31. Carrascosa PM, Cury RC, Deviggiano A, Capunay C, Campisi R, López de Munain M, et al. Comparison of myocardial perfusion evaluation with single versus dual-energy CT and effect of beam-hardening artifacts. *Acad Radiol* 2015;22:591-599
32. Pelgrim GJ, van Hamersvelt RW, Willemink MJ, Schmidt BT, Flohr T, Schilham A, et al. Accuracy of iodine quantification using dual energy CT in latest generation dual source and dual layer CT. *Eur Radiol* 2017;27:3904-3912
33. Delgado Sánchez-Gracián C, Oca Pernas R, Trinidad López C, Santos Armentia E, Vaamonde Liste A, Vázquez Caamaño M, et al. Quantitative myocardial perfusion with stress dual-energy CT: iodine concentration differences between normal and ischemic or necrotic myocardium. Initial experience. *Eur Radiol* 2016;26:3199-3207
34. Nagao M, Matsuoka H, Kawakami H, Higashino H, Mochizuki T, Uemura M, et al. Myocardial ischemia in acute coronary syndrome: assessment using 64-MDCT. *AJR Am J Roentgenol* 2009;193:1097-1106
35. Rossi A, Dharampal A, Wragg A, Davies LC, van Geuns RJ, Anagnostopoulos C, et al. Diagnostic performance of hyperaemic myocardial blood flow index obtained by dynamic computed tomography: does it predict functionally significant coronary lesions? *Eur Heart J Cardiovasc Imaging* 2014;15:85-94
36. Conte E, Sonck J, Mushtaq S, Collet C, Mizukami T, Barbato E, et al. FFRCT and CT perfusion: a review on the evaluation of functional impact of coronary artery stenosis by cardiac CT. *Int J Cardiol* 2020;300:289-296
37. Lubbers M, Coenen A, Kofflard M, Bruning T, Kietselaer B, Galema T, et al. Comprehensive cardiac CT with myocardial perfusion imaging versus functional testing in suspected coronary artery disease: the multicenter, randomized CRESCENT-II trial. *JACC Cardiovasc Imaging* 2018;11:1625-1636
38. Bamberg F, Hinkel R, Schwarz F, Sandner TA, Baloch E, Marcus R, et al. Accuracy of dynamic computed tomography adenosine stress myocardial perfusion imaging in estimating myocardial blood flow at various degrees of coronary artery stenosis using a porcine animal model. *Invest Radiol* 2012;47:71-77
39. George RT, Jerosch-Herold M, Silva C, Kitagawa K, Bluemke DA, Lima JA, et al. Quantification of myocardial perfusion using dynamic 64-detector computed tomography. *Invest Radiol* 2007;42:815-822
40. Bamberg F, Becker A, Schwarz F, Marcus RP, Greif M, von Ziegler F, et al. Detection of hemodynamically significant coronary artery stenosis: incremental diagnostic value of dynamic CT-based myocardial perfusion imaging. *Radiology* 2011;260:689-698
41. Huber AM, Leber V, Gramer BM, Muenzel D, Leber A, Rieber J, et al. Myocardium: dynamic versus single-shot CT perfusion imaging. *Radiology* 2013;269:378-386
42. Pontone G, Baggiano A, Andreini D, Guaricci AI, Guglielmo M, Muscogiuri G, et al. Dynamic stress computed tomography perfusion with a whole-heart coverage scanner in addition to coronary computed tomography angiography and fractional flow reserve computed tomography derived. *JACC Cardiovasc Imaging* 2019;12:2460-2471
43. Li Y, Dai X, Lu Z, Shen C, Zhang J. Diagnostic performance of quantitative, semi-quantitative, and visual analysis of dynamic CT myocardial perfusion imaging: a validation study

 https://doi.org/10.3348/kjr.2020.1277

with invasive fractional flow reserve. *Eur Radiol* 2021;31:525-534
44. Pontone G, Baggiano A, Andreini D, Guaricci AI, Guglielmo M, Muscogiuri G, et al. Diagnostic accuracy of simultaneous evaluation of coronary arteries and myocardial perfusion with single stress cardiac computed tomography acquisition compared to invasive coronary angiography plus invasive fractional flow reserve. *Int J Cardiol* 2018;273:263-268
45. Li Y, Yu M, Dai X, Lu Z, Shen C, Wang Y, et al. Detection of hemodynamically significant coronary stenosis: CT myocardial perfusion versus machine learning CT fractional flow reserve. *Radiology* 2019;293:305-314
46. Fahmi R, Eck BL, Levi J, Fares A, Wu H, Vembar M, et al. Effect of beam hardening on transmural myocardial perfusion quantification in myocardial CT imaging. *Proc SPIE Int Soc Opt Eng* 2016;9788:97882I
47. Yi Y, Xu C, Wu W, Shen ZJ, Lee W, Yun CH, et al. Low-dose CT perfusion with combined use of CTP and CTP-derived coronary CT angiography at 70 kVp: validation with invasive fractional flow reserve. *Eur Radiol* 2020;31:1119-1129
48. Min JK, Taylor CA, Achenbach S, Koo BK, Leipsic J, Nørgaard BL, et al. Noninvasive fractional flow reserve derived from coronary CT angiography: clinical data and scientific principles. *JACC Cardiovasc Imaging* 2015;8:1209-1222
49. Koo BK, Erglis A, Doh JH, Daniels DV, Jegere S, Kim HS, et al. Diagnosis of ischemia-causing coronary stenoses by noninvasive fractional flow reserve computed from coronary computed tomographic angiograms. Results from the prospective multicenter DISCOVER-FLOW (Diagnosis of Ischemia-Causing Stenoses Obtained Via Noninvasive Fractional Flow Reserve) study. *J Am Coll Cardiol* 2011;58:1989-1997
50. Coenen A, Lubbers MM, Kurata A, Kono A, Dedic A, Chelu RG, et al. Fractional flow reserve computed from noninvasive CT angiography data: diagnostic performance of an on-site clinician-operated computational fluid dynamics algorithm. *Radiology* 2015;274:674-683
51. Tang CX, Liu CY, Lu MJ, Schoepf UJ, Tesche C, Bayer RR 2nd, et al. CT FFR for ischemia-specific CAD with a new computational fluid dynamics algorithm: a Chinese multicenter study. *JACC Cardiovasc Imaging* 2020;13:980-990
52. Qiao HY, Li JH, Schoepf UJ, Bayer RR, Tinnefeld FC, Di Jiang M, et al. Prognostic implication of CT-FFR based functional SYNTAX score in patients with de novo three-vessel disease. *Eur Heart J Cardiovasc Imaging* 2020 Nov [Epub]. https://doi.org/10.1093/ehjci/jeaa256
53. Kim SH, Kang SH, Chung WY, Yoon CH, Park SD, Nam CW, et al. Validation of the diagnostic performance of 'HeartMedi V.1.0', a novel CT-derived fractional flow reserve measurement, for patients with coronary artery disease: a study protocol. *BMJ Open* 2020;10:e037780
54. Wang ZQ, Zhou YJ, Zhao YX, Shi DM, Liu YY, Liu W, et al. Diagnostic accuracy of a deep learning approach to calculate FFR from coronary CT angiography. *J Geriatr Cardiol* 2019;16:42-48
55. Nørgaard BL, Leipsic J, Gaur S, Seneviratne S, Ko BS, Ito H, et al. Diagnostic performance of noninvasive fractional flow reserve derived from coronary computed tomography angiography in suspected coronary artery disease: the NXT trial (analysis of coronary blood flow using CT angiography: next steps). *J Am Coll Cardiol* 2014;63:1145-1155
56. Cook CM, Petraco R, Shun-Shin MJ, Ahmad Y, Nijjer S, Al-Lamee R, et al. Diagnostic accuracy of computed tomography–derived fractional flow reserve: a systematic review. *JAMA Cardiol* 2017;2:803-810
57. Fairbairn TA, Nieman K, Akasaka T, Nørgaard BL, Berman DS, Raff G, et al. Real-world clinical utility and impact on clinical decision-making of coronary computed tomography angiography-derived fractional flow reserve: lessons from the ADVANCE Registry. *Eur Heart J* 2018;39:3701-3711
58. Fujimoto S, Kawasaki T, Kumamaru KK, Kawaguchi Y, Dohi T, Okonogi T, et al. Diagnostic performance of on-site computed CT-fractional flow reserve based on fluid structure interactions: comparison with invasive fractional flow reserve and instantaneous wave-free ratio. *Eur Heart J Cardiovasc Imaging* 2019;20:343-352
59. Siogkas PK, Anagnostopoulos CD, Liga R, Exarchos TP, Sakellarios AI, Rigas G, et al. Noninvasive CT-based hemodynamic assessment of coronary lesions derived from fast computational analysis: a comparison against fractional flow reserve. *Eur Radiol* 2019;29:2117-2126
60. Min JK, Leipsic J, Pencina MJ, Berman DS, Koo BK, van Mieghem C, et al. Diagnostic accuracy of fractional flow reserve from anatomic CT angiography. *JAMA* 2012;308:1237-1245
61. Nørgaard BL, Gaur S, Leipsic J, Ito H, Miyoshi T, Park SJ, et al. Influence of coronary calcification on the diagnostic performance of CT angiography derived FFR in coronary artery disease: a substudy of the NXT trial. *JACC Cardiovasc Imaging* 2015;8:1045-1055
62. Tesche C, Otani K, De Cecco CN, Coenen A, De Geer J, Kruk M, et al. Influence of coronary calcium on diagnostic performance of machine learning CT-FFR: results from MACHINE registry. *JACC Cardiovasc Imaging* 2020;13:760-770
63. Di Jiang M, Zhang XL, Liu H, Tang CX, Li JH, Wang YN, et al. The effect of coronary calcification on diagnostic performance of machine learning-based CT-FFR: a Chinese multicenter study. *Eur Radiol* 2021;31:1482-1493
64. Pontone G, Baggiano A, Andreini D, Guaricci AI, Guglielmo M, Muscogiuri G, et al. Stress computed tomography perfusion versus fractional flow reserve CT derived in suspected coronary artery disease: the PERFECTION study. *JACC Cardiovasc Imaging* 2019;12:1487-1497
65. Nakazato R, Park HB, Berman DS, Gransar H, Koo BK, Erglis A, et al. Noninvasive fractional flow reserve derived from computed tomography angiography for coronary lesions of intermediate stenosis severity: results from the DeFACTO study. *Circ Cardiovasc Imaging* 2013;6:881-889

66. Min JK, Koo BK, Erglis A, Doh JH, Daniels DV, Jegere S, et al. Usefulness of noninvasive fractional flow reserve computed from coronary computed tomographic angiograms for intermediate stenoses confirmed by quantitative coronary angiography. *Am J Cardiol* 2012;110:971-976
67. Donnelly PM, Kolossváry M, Karády J, Ball PA, Kelly S, Fitzsimons D, et al. Experience with an on-site coronary computed tomography-derived fractional flow reserve algorithm for the assessment of intermediate coronary stenoses. *Am J Cardiol* 2018;121:9-13
68. Nakamura S, Kitagawa K, Goto Y, Omori T, Kurita T, Yamada A, et al. Incremental prognostic value of myocardial blood flow quantified with stress dynamic computed tomography perfusion imaging. *JACC Cardiovasc Imaging* 2019;12:1379-1387
69. Chen MY, Rochitte CE, Arbab-Zadeh A, Dewey M, George RT, Miller JM, et al. Prognostic value of combined CT angiography and myocardial perfusion imaging versus invasive coronary angiography and nuclear stress perfusion imaging in the prediction of major adverse cardiovascular events: the CORE320 multicenter study. *Radiology* 2017;284:55-65
70. Douglas PS, De Bruyne B, Pontone G, Patel MR, Norgaard BL, Byrne RA, et al. 1-year outcomes of FFRCT-guided care in patients with suspected coronary disease: the PLATFORM study. *J Am Coll Cardiol* 2016;68:435-445
71. Leipsic J, Yang TH, Thompson A, Koo BK, Mancini GB, Taylor C, et al. CT angiography (CTA) and diagnostic performance of noninvasive fractional flow reserve: results from the Determination of Fractional Flow Reserve by Anatomic CTA (DeFACTO) study. *AJR Am J Roentgenol* 2014;202:989-994
72. Ri K, Kumamaru KK, Fujimoto S, Kawaguchi Y, Dohi T, Yamada S, et al. Noninvasive computed tomography–derived fractional flow reserve based on structural and fluid analysis: reproducibility of on-site determination by unexperienced observers. *J Comput Assist Tomogr* 2018;42:256-262
73. Tesche C, De Cecco CN, Baumann S, Renker M, McLaurin TW, Duguay TM, et al. Coronary CT angiography–derived fractional flow reserve: machine learning algorithm versus computational fluid dynamics modeling. *Radiology* 2018;288:64-72
74. Zreik M, Lessmann N, van Hamersvelt RW, Wolterink JM, Voskuil M, Viergever MA, et al. Deep learning analysis of the myocardium in coronary CT angiography for identification of patients with functionally significant coronary artery stenosis. *Med Image Anal* 2018;44:72-85
75. Kumamaru KK, Fujimoto S, Otsuka Y, Kawasaki T, Kawaguchi Y, Kato E, et al. Diagnostic accuracy of 3D deep-learning-based fully automated estimation of patient-level minimum fractional flow reserve from coronary computed tomography angiography. *Eur Heart J Cardiovasc Imaging* 2020;21:437-445
76. Agostini D, Roule V, Nganoa C, Roth N, Baavour R, Parienti JJ, et al. First validation of myocardial flow reserve assessed by dynamic 99mTc-sestamibi CZT-SPECT camera: head to head comparison with 15O-water PET and fractional flow reserve in patients with suspected coronary artery disease. The WATERDAY study. *Eur J Nucl Med Mol Imaging* 2018;45:1079-1090
77. Pontone G, Andreini D, Guaricci AI, Guglielmo M, Baggiano A, Muscogiuri G, et al. Quantitative vs. qualitative evaluation of static stress computed tomography perfusion to detect haemodynamically significant coronary artery disease. *Eur Heart J Cardiovasc Imaging* 2018;19:1244-1252
78. Bettencourt N, Chiribiri A, Schuster A, Ferreira N, Sampaio F, Pires-Morais G, et al. Direct comparison of cardiac magnetic resonance and multidetector computed tomography stress-rest perfusion imaging for detection of coronary artery disease. *J Am Coll Cardiol* 2013;61:1099-107
79. Coenen A, Rossi A, Lubbers MM, Kurata A, Kono AK, Chelu RG, et al. Integrating CT myocardial perfusion and CT-FFR in the work-up of coronary artery disease. *JACC Cardiovasc Imaging* 2017;10:760-770
80. Rossi A, Wragg A, Klotz E, Pirro F, Moon JC, Nieman K, et al. Dynamic computed tomography myocardial perfusion imaging: comparison of clinical analysis methods for the detection of vessel-specific ischemia. *Circ Cardiovasc Imaging* 2017;10:e005505
81. Kono AK, Coenen A, Lubbers M, Kurata A, Rossi A, Dharampal A, et al. Relative myocardial blood flow by dynamic computed tomographic perfusion imaging predicts hemodynamic significance of coronary stenosis better than absolute blood flow. *Invest Radiol* 2014;49:801-807
82. Greif M, von Ziegler F, Bamberg F, Tittus J, Schwarz F, D'Anastasi M, et al. CT stress perfusion imaging for detection of haemodynamically relevant coronary stenosis as defined by FFR. *Heart* 2013;99:1004-1011
83. Coenen A, Kim YH, Kruk M, Tesche C, De Geer J, Kurata A, et al. Diagnostic accuracy of a machine-learning approach to coronary computed tomographic angiography–based fractional flow reserve: result from the MACHINE consortium. *Circ Cardiovasc Imaging* 2018;11:e007217
84. Ko BS, Cameron JD, Munnur RK, Wong DTL, Fujisawa Y, Sakaguchi T, et al. Noninvasive CT-derived FFR based on structural and fluid analysis: a comparison with invasive FFR for detection of functionally significant stenosis. *JACC Cardiovasc Imaging* 2017;10:663-673
85. Chung JH, Lee KE, Nam CW, Doh JH, Kim HI, Kwon SS, et al. Diagnostic performance of a novel method for fractional flow reserve computed from noninvasive computed tomography angiography (NOVEL-FLOW Study). *Am J Cardiol* 2017;120:362-368
86. Melikian N, De Bondt P, Tonino P, De Winter O, Wyffels E, Bartunek J, et al. Fractional flow reserve and myocardial perfusion imaging in patients with angiographic multivessel coronary artery disease. *JACC Cardiovasc Interv* 2010;3:307-314

 https://doi.org/10.3348/kjr.2020.1277